Inorg. Chem. **2009**, *48*, 1398−1406

An Acyclic Dimer of Cyclodiphosphazane $\{^t$BuHN(^{t}BuNP)$_2$OCH$_2\}_2$ Containing Alkoxo and Amido Functionalities: Synthesis, Derivatization, Bi- (Pd^{II}, Rh^I), and Tetranuclear (Pd^{II}, Au^I, Rh^IAu^I) Transition Metal Complexes

Maravanji S. Balakrishna,*,† Ramalingam Venkateswaran,† and Joel T. Mague‡

Phosphorus Laboratory, Department of Chemistry, Indian Institute of Technology Bombay, Mumbai 400 076, India, and Tulane University, New Orleans, Louisiana 70118

Received July 24, 2008

Acyclic bis(cyclodiphosphazane) [^{t}BuHN(^{t}BuNP)$_2$OCH$_2$]$_2$ (**2**) containing alkoxo and amido functionalities was synthesized by reacting *cis*-[^{t}BuHN(^{t}BuNP)$_2$Cl] (**1**) with ethylene glycol and upon further treatment with 4 equiv of elemental sulfur or selenium affords the corresponding tetrachalcogenides [^{t}BuHN(^{t}BuNPE)$_2$OCH$_2$]$_2$ (**3**, E = S; **4**, E = Se) in quantitative yield. The reaction of **2** with 2 equiv of elemental sulfur results in the oxidation of only the amido-phosphorus atoms to form the di(sulfide) derivative [^{t}BuHN(S)P(μ-^{t}BuN)POCH$_2$]$_2$ (**5**). The reaction of **2** with 2 equiv of [PdCl(η^3-C$_3$H$_5$)]$_2$ afforded the tetrametallic complex [{Pd(η^3-allyl)Cl}$_4${^{t}BuHN(^{t}BuNP)$_2$OCH$_2$}$_2$] (**7**) containing four independent [PdCl$_2$(η^3-C$_3$H$_5$)] moieties each coordinated to a phosphorus atom. In contrast, the reaction between [Pd(PEt$_3$)Cl$_2$]$_2$ and **2** leads to the addition of two metal atoms with the formation of [{Pd(PEt$_3$)Cl}$_2$-{^{t}BuHN(^{t}BuNP)$_2$OCH$_2$}$_2$] (**8**), in which alternating phosphorus atoms of the bis(cyclodiphosphazane) are coordinated to palladium. Interestingly, the palladium(II) atom coordinated to the phosphorus atom bearing the *t*-butylamino substituent adopts a trans geometry, whereas that coordinated to the phosphorus atom connected to the −OCH$_2$CH$_2$O− linker prefers a cis conformation. The reaction between **2** and [Rh(COD)Cl]$_2$ produces exclusively the bimetallic complex [{Rh(COD)Cl}$_2${^{t}BuHN(^{t}BuNP)$_2$OCH$_2$}$_2$] (**6**) irrespective of the stoichiometry of the reactants and the reaction conditions. In complex **6**, only the alkoxo-phosphorus atoms are coordinated. However, complex **6** upon treatment with AuCl(SMe$_2$) in a 1:2 ratio gives the heterometallic tetrasubstituted complex [{Rh(COD)Cl}$_2$(AuCl)$_2${^{t}BuHN(^{t}BuNP)$_2$OCH$_2$}$_2$] (**10**). The reaction between 4 equiv of AuCl(SMe$_2$) and **2** resulted in the formation of a tetrametallic gold complex [(AuCl)$_4${^{t}BuHN(^{t}BuNP)$_2$OCH$_2$}$_2$] (**9**). The crystal structures of **2**−**4** and **7**−**10** are reported.

Introduction

The renewed interest in the chemistry[1,2] of cyclodiphosphazanes or diazadiphosphetidines in recent years is due to the use of robust P_2N_2 skeletons as building blocks to make a variety of cages, clusters, and macrocycles as well as their interesting ligating behavior both as neutral[3] and as anionic ligands[4−6] and also their catalytic[7] and biological applications.[8] The reactions between the simplest cyclodiphosphazane, [ClP(μ-NR)]$_2$, and diols, diamines, or amine-alcohols

* To whom correspondence should be addressed. Tel.: +91 22 2576 7181. Fax: +91 22 2576 7152/2572 3480. E-mail: krishna@chem.iitb.ac.in.
† Indian Institute of Technology Bombay.
‡ Tulane University.

(1) Balakrishna, M. S.; Eisler, D. J.; Chivers, T. *Chem. Soc. Rev.* **2007**, *36*, 650–664.
(2) Burford, N.; Cameron, T. S.; Conroy, K. D.; Ellis, B.; Lumsden, M.; Macdonald, C. L. B.; McDonald, R.; Phillips, A. D.; Ragogna, P. J.; Schurko, R. W.; Walsh, D.; Wasylishen, R. E. *J. Am. Chem. Soc.* **2002**, *124*, 14012–14013.
(3) (a) Chandrasekaran, P.; Mague, J. T.; Balakrishna, M. S. *Organometallics* **2005**, *24*, 3780–3783. (b) Chandrasekaran, P.; Mague, J. T.; Balakrishna, M. S. *Inorg. Chem.* **2006**, *45*, 6678–6683. (c) Chandrasekaran, P.; Mague, J. T.; Balakrishna, M. S. *Inorg. Chem.* **2006**, *45*, 5893–5897. (d) Chandrasekaran, P. Ph.D. Thesis, Indian Institute of Technology Bombay, Mumbai, India, 2006. (e) Balakrishna, M. S.; Mague, J. T. *Organometallics* **2007**, *26*, 4677–4679. (f) Suresh, D.; Balakrishna, M. S.; Mague, J. T. *Dalton Trans.* **2008**, 3272–3274. (g) Suresh, D.; Balakrishna, M. S.; Mague, J. T. *Tetrahedron Lett.* **2007**, *48*, 2283–2285. (h) Chandrasekaran, P.; Mague, J. T.; Balakrishna, M. S. *Tetrahedron Lett.* **2007**, *48*, 5227–5229. (i) Balakrishna, M. S.; Chandrasekaran, P.; Ventakeswaran, R. *J. Organomet. Chem.* **2007**, *48*, 5227–5229.

10.1021/ic801256h CCC: $40.75
Published on Web 01/09/2009

resulted in the formation of simple monomeric derivatives[9] and dimeric−pentameric macrocycles,[10−13] whereas only a very few reactions have yielded mono- or disubstituted derivatives. Surprisingly, the reports of the synthesis of simple acyclic dimers of cyclodiphosphazanes or bis(cyclodiphosphazanes) are scarce[14,15] despite the availability of the synthetically useful monochloro derivative, [ClP(μ-NR)$_2$PN(H)^{t}Bu]. Although, a few dimers of cyclodiphosphazanes with acyclic structure are known,[16,17,14] there are no reports on further reactivity or their utility as neutral or anionic ligands in coordination chemistry. This prompted us to prepare acyclic dimers, trimers, or polymers of the type [{^{t}BuHN(^{t}BuNP)$_2$}$_n${Q}$_{n-1}$], containing amido and alkoxo functionalities to assess their coordination behavior as both neutral and anionic ligands. Herein, we report the synthesis, reactivity, and di- and tetranuclear late transition metal complexes of bis(cyclodiphosphazane), {^{t}BuHN(^{t}BuNP)$_2$OCH$_2$}$_2$.

Results and Discussion

Synthesis of {^{t}BuHN(^{t}BuNP)$_2$OCH$_2$}$_2$ (2) and Chalcogen Derivatives. The alkoxy-bridged bis(cyclodiphosphazane) {^{t}BuHN(^{t}BuNP)$_2$OCH$_2$}$_2$ (**2**) has been synthesized from the reaction of ethylene glycol with 2 equiv of monochloro-derivative *cis*-{^{t}BuHN(^{t}BuNP)$_2$Cl} (**1**) and triethylamine in diethyl ether at 0 °C. Compound **2** is obtained as a white solid and is moderately stable to air and moisture, both in the solution and in the solid state. The ^{31}P NMR spectrum of **2** exhibits two resonances at 92.4 (s) and 112.7 (s) ppm, respectively, for amido-P (hereafter "outer") and alkoxo-P (hereafter "inner") atoms. The ^{1}H NMR spectrum confirms the presence of two CH_2 groups; the resonance due to which appears at 3.84 ppm. The mass spectrum of **2** shows a molecular ion $[M + 1]^+$ peak at 613.69 *m*/*z*. The structure of compound **2** has been confirmed by single-crystal X-ray diffraction study.

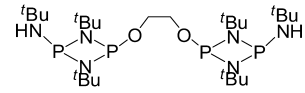

2

Treatment of **2** with 4 equiv of elemental sulfur or selenium in toluene under refluxing conditions resulted in the formation of the tetrathio and tetraselenoyl derivatives, {^{t}BuHN(^{t}BuNP(S))$_2$OCH$_2$}$_2$ (**3**) and {^{t}BuHN(^{t}BuNP(Se))$_2$OCH$_2$}$_2$ (**4**), respectively, in good yield. The phosphorus-31 NMR spectrum of **3** shows two doublets centered at 37.5 and 51.4 ppm with a $^2J_{PP}$ value of 32.4 Hz. Similarly, compound **4** also exhibits two doublets at 24.4 and 45.8 ppm with a $^2J_{PP}$ coupling of 16.7 Hz, and each shows satellites with $^1J_{SeP}$ couplings of 895 and 937 Hz, respectively. The $^1J_{SeP}$ coupling constants are comparable to those of *cis*-{^{t}BuNP(Se)(NHCy)}$_2$ ($^1J_{SeP}$ = 878 Hz) and *cis*-{^{t}BuNP(Se)(OCH$_2$CH$_2$OMe)}$_2$ ($^1J_{SeP}$ = 953 Hz).[3d] Mass spectral and microanalysis data support the compositions of compounds **3** and **4**, and the structures are confirmed by single-crystal X-ray diffraction studies.

The reaction of 2 equiv of elemental selenium with **2** in toluene at room temperature affords diselenide {^{t}BuHN(^{t}BuNP)$_2$OCH$_2$}$_2$(Se)$_2$ (**5**), whereas the attempts to synthesize the corresponding disulfide have been unsuccessful and resulted in the formation of a statistical mixture of products which could not be characterized. Compound **5** has been isolated as a white solid in good yield. The ^{31}P NMR spectrum of **5** exhibits two resonances at 78.6 and 46.0 ppm, with the latter showing satellites with a $^1J_{SeP}$ coupling of 874 Hz. This indicates that the outer P(III) centers are susceptible to initial oxidation with selenium rather than the inner phosphorus centers as expected due to the greater Lewis basicity of the former. The formulation of compound **5** has been confirmed from the mass spectrometry, which shows a molecular ion peak at *m*/*z* 772.8.

Although the geometry and the coordination modes are unpredictable in the complexation reactions, it is not all that difficult to guess the nature of the complexes obtained with platinum metals by looking into the previous reports.[3] For example, the interaction of dimeric cyclodiphosphazane with chalcogens gives either terminal P-oxidized or a completely oxidized product depending on the stoichiometry, which is obvious due to the difference in the basicity of phosphorus centers with terminals being relatively more basic. Similarly, there is a marked variation in their π-acceptor ability, with terminal phosphorus centers being relatively weak π-acceptors compared to the glycol-substituted phosphorus centers. Metals in their low valent state prefer to coordinate to the inner phosphorus centers unless there is a steric objection. Hence, the coordinating ability of this ligand is under the influence of both steric and electronic attributes. The metal chemistry reported in this paper has been considered under these aspects.

Synthesis of Transition Metal Complexes of 2. Treatment of **2** with [Rh(COD)Cl]$_2$ in dichloromethane afforded

(4) Stahl, L. *Coord. Chem. Rev.* **2000**, *210*, 203–250.
(5) Briand, G. G.; Chivers, T.; Krahn, M. *Coord. Chem. Rev.* **2002**, *233−234*, 237–254.
(6) Lief, G. R.; Moser, D. F.; Stahl, L.; Staples, R. J. *J. Organomet. Chem.* **2004**, *689*, 1110–1121.
(7) (a) Moser, D. F.; Grocholl, L.; Stahl, L.; Staples, R. J. *J. Chem. Soc., Dalton Trans.* **2003**, 1402–1410. (b) Axenov, K. V.; Leskelä, M.; Repo, T. *J. Catal.* **2006**, *238*, 196–205. (c) Axenov, K. V.; Klinga, M.; Leskela, M.; Repo, T. *Organometallics* **2005**, *24*, 1336–1343.
(8) Suresh, D.; Balakrishna, M. S.; Rathinasamy, K.; Panda, D.; Mobin, S. M. *Dalton Trans.* **2008**, 2812−2814.
(9) Kumaravel, S. S.; Krishnamurthy, S. S.; Cameron, T. S.; Linden, A. *Inorg. Chem.* **1988**, *27*, 4546–4550.
(10) Brask, J. K.; Chivers, T.; Krahn, M. L.; Parvez, M. *Inorg. Chem.* **1999**, *38*, 290–295.
(11) Garcia, F.; Kowenicki, R. A.; Kuzu, I.; Riera, L.; McPartlin, M.; Wright, D. S. *J. Chem. Soc., Dalton Trans.* **2004**, 2904–2909.
(12) Garcia, F.; Goodman, J. M.; Kowenicki, R. A.; Kuzu, I.; McPartlin, M.; Silva, M. A.; Riera, L.; Woods, A. D.; Wright, D. S. *Chem.−Eur. J.* **2004**, *10*, 6066–6072.
(13) Bashall, A.; Doyle, E. L.; Tubb, C.; Kidd, S. J.; McPartlin, M.; Woods, A. D.; Wright, D. S. *Chem. Commun.* **2001**, 2542–2543.
(14) Kommana, P.; Kumara Swamy, K. C. *Inorg. Chem.* **2000**, *39*, 4384–4385.
(15) Kommanna, P.; Vittal, J. J.; Kumara Swamy, K. C. *Polyhedron* **2003**, *22*, 843–947.
(16) Doyle, E. L.; Garcia, F.; Humprey, S. M.; Kowenicki, R. A.; Riera, L.; Woods, A. D.; Wright, D. S. *J. Chem. Soc., Dalton Trans.* **2004**, 807–812.
(17) Thompson, M. L.; Haltiwanger, R. C.; Norman, A. D. *J. Chem. Soc., Chem. Commun.* **1979**, 379–280.

exclusively the dimetallic Rh^I complex $[\{Rh(COD)Cl\}_2\{^tBuHN(^tBuNP)_2OCH_2\}_2]$ (**6**) irrespective of the reaction stoichiometry and the reaction conditions. The addition of an excess of metal reagent did not afford the expected tetrametallic rhodium complex. The ^{31}P NMR spectrum of complex **6** presents two resonances at 90.8 (s) and 91.9 (d) ppm with a J_{RhP} coupling of 219.3 Hz, which clearly indicates the coordination of the inner phosphorus atoms while the outer phosphorus centers remain uncoordinated. The ES ionization mass spectrum shows the $[M + 1]^+$ peak at 1105.30 *m/z*. The ^1H NMR spectrum confirms the presence of cyclooctadienyl protons, which exhibit resonances at 2.09, 2.34, 3.81, and 5.51 ppm.

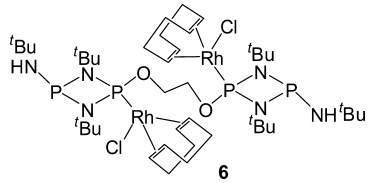

6

The reaction of **2** with $[Pd(\eta^3\text{-allyl})Cl]_2$ in a 1:2 molar ratio in dichloromethane leads to the formation of $[\{Pd(\eta^3\text{-allyl})Cl\}_4\{^tBuHN(^tBuNP)_2OCH_2\}_2]$ (**7**) in quantitative yield. This is a rare example having four Pd(π-allyl)Cl moieties in a single molecule without any metal−metal interaction. The ^{31}P NMR spectrum of complex **7** exhibits four resonances at 118.6 (s), 118.4 (s), 77.6 (s), and 76.4 (s) ppm, which indicates that all four phosphorus centers are magnetically nonequivalent. Surprisingly, the phosphorus−phosphorus coupling was not observed. The high-frequency chemical shifts are assigned to the inner phosphorus centers. The presence of η^3-allyl groups has been confirmed from the ^1H NMR spectrum, which shows broad peaks in the range 3.57−5.64 ppm.

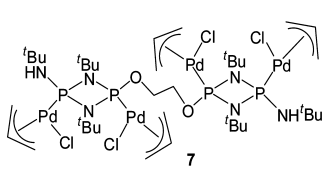

7

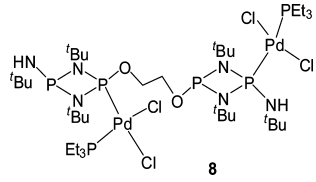

8

The dimetallic Pd^{II} complex $[\{Pd(PEt_3)Cl\}_2\{^tBuHN(^tBuNP)_2OCH_2\}_2]$ (**8**) has been synthesized from the reaction of **2** with $[Pd(PEt_3)Cl_2]_2$ in a 1:1 molar ratio at room temperature. The addition of an excess of palladium reagent also resulted in the formation of the same dimetallic complex **8**. The ^{31}P NMR spectrum of complex **8** consists of six resonances which can be readily assigned. The splitting pattern suggests that one of the Pd^{II} centers is bound to an inner phosphorus atom, while the other Pd^{II} is connected to an outer phosphorus atom. The signals due to PEt_3 appear at 20.2 (dd) and 29.3 (d) ppm. The large $^2J_{PP}$ coupling (711 Hz) associated with the doublet of doublets at 20.2 ppm indicates a trans disposition[18] of PEt_3 with respect to the outer phosphorus center, which resonates at 126.9 ppm. The *trans*-PEt_3 center is also coupled to the uncoordinated inner phosphorus center ($^5J_{PP} = 8.9$ Hz), with the resonance due to the latter appearing as a doublet of doublets at 126.9 ppm, indicating its noncoordinated nature. The resonance at 29.3 shows a $^2J_{PP}$ coupling of 14.6 Hz, indicating its cis relationship with the coordinated inner phosphorus atom, which resonates as a doublet of doublet at 72.8 ppm, with the other $^2J_{PP}$ coupling of 7.8 Hz being due to its coupling with the uncoordinated outer phosphorus atom. The last resonates at 92 ppm as a doublet with a $^2J_{PP}$ coupling of 7.8 Hz.

The two PEt_3 groups are present in different chemical environments, which is further confirmed from the ^1H NMR data, which consists of two separate sets of resonances for ethylene groups at 1.16 (t, *Et*, 9H), 1.20 (t, *Et*, 9H), 1.86 (m, *Et*, 6H), and 2.07 (m, *Et*, 6H) ppm. The molecular structure of complex **8** has been confirmed from the single-crystal X-ray diffraction study.

The 1:4 reaction of **2** with $[AuCl(SMe_2)]$ in dichloromethane affords a tetrametallic Au^I complex $[(AuCl)_4\{^tBuHN(^tBuNP)_2OCH_2\}_2]$ (**9**) as pale yellow crystals. Complex **9** is insoluble in most of the organic solvents, which prevents the ability to perform solution NMR studies. However, the microanalysis data for **9** adequately support the proposed composition, and this has been further confirmed by a single-crystal X-ray study.

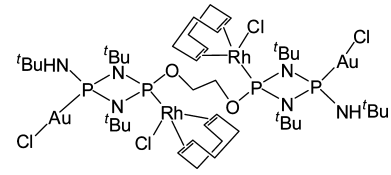

10

The reaction of complex **6** with 2 equiv of $[AuCl(SMe_2)]$ in dichloromethane at room temperature afforded the heterometallic $2Rh^I/2Au^I$ complex $[\{Rh(COD)Cl\}_2(AuCl)_2\{^tBuHN(^tBuNP)_2OCH_2\}_2]$ (**10**) in good yield. Solution spectroscopic studies on complex **10** could not be carried out because of its poor solubility in most organic solvents. However, the elemental analysis and mass spectral data confirm the chemical composition of **10**, and the structure of **10** has been established from a single-crystal X-ray diffraction study.

Molecular Structures of Compounds 2−4 and 7−10. The molecular structures of compounds **2**−**4** and **7**−**10** are shown in Figures 1−7, with crystallographic information given in Table 1 and selected geometric parameters given in Tables 2−5. The structures of the new compound **2** and its disulfide and diselenide derivatives **3** and **4** are composed of two P_2N_2 rings that are bridged by a $-OCH_2CH_2O-$ linker. Molecule **2** has approximate 2-fold rotational symmetry centered about the midpoint of the C13−C14 bond. Compounds **3** and **4** are isostructural with three molecules in the unit cell. One of these has crystallographically imposed centrosymmetry, while the other has no imposed symmetry. In the case of **4**, this latter molecule shows an 84:16 disorder in the CH_2CH_2 portion of the linker.

Unsymmetrically substituted cyclodiphosphazanes show unequal endocylic P−N bond distances with longer P−N

(18) Baenziger, N. C.; Bennett, W. E.; Soboroff, D. M. *Acta Crystallogr.* **1976**, *B32*, 2547–2553.

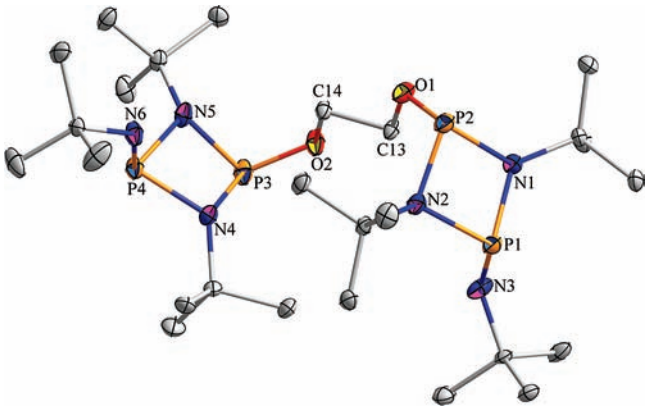

Figure 1. Molecular structure of {^{t}BuHN(^{t}BuNP)$_2$OCH$_2$}$_2$ (**2**). Thermal ellipsoids are drawn at the 50% probability level. Hydrogen atoms have been omitted for clarity. Only one orientation of the disordered *tert*-butyl group is shown.

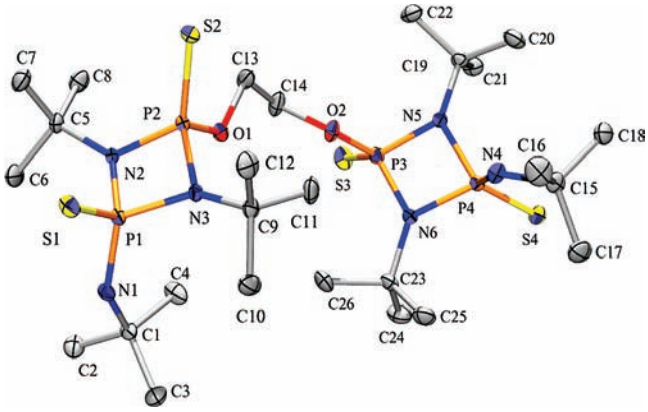

Figure 2. Molecular structure of {^{t}BuHN(^{t}BuNP(S))$_2$OCH$_2$}$_2$ (**3**). Thermal ellipsoids are drawn at the 50% probability level. Hydrogen atoms have been omitted for clarity.

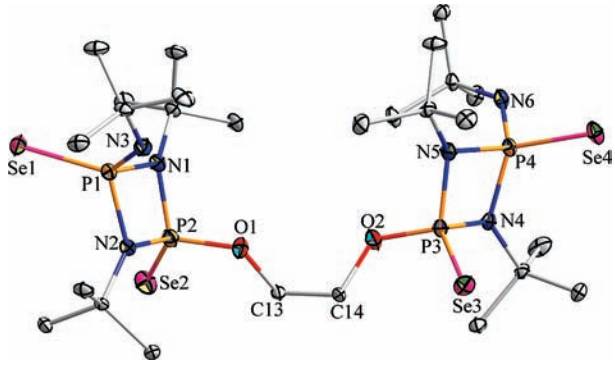

Figure 3. Molecular structure of {^{t}BuHN(^{t}BuNP(Se))$_2$OCH$_2$}$_2$ (**4**). Thermal ellipsoids are drawn at the 50% probability level. Hydrogen atoms have been omitted for clarity. Only one orientation of the disordered portion of the molecule is shown.

bonds associated with the phosphorus atom having exocyclic nitrogen substituents and shorter P−N bonds with those bearing oxo, alkoxy, aryloxy, or halo substituents. In cyclodiphosph(III)azanes containing trivalent phosphorus centers, this difference may not be remarkable, but in cyclodiphosph(V)azans, the difference is quite considerable, as seen in compound **2** versus **3** and **4** in the present investigation. The exocyclic P−N distances are always shorter and comparable with typical P−N distances observed

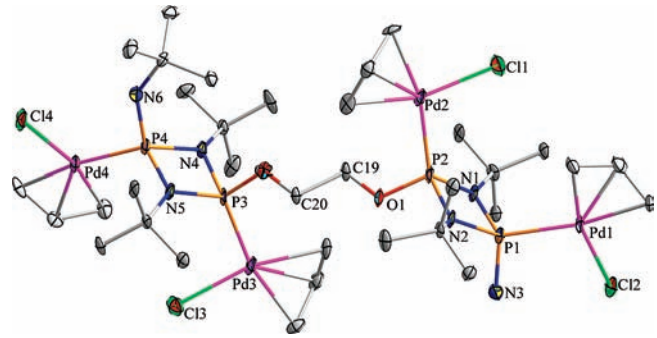

Figure 4. Molecular structure of complex [{Pd(π-allyl)Cl}$_4${^{t}BuHN(^{t}BuNP)$_2$OCH$_2$}$_2$] (**7**). Thermal ellipsoids are drawn at the 50% probability level. Hydrogen atoms have been omitted for clarity. Only one orientation of the disordered allyl groups is shown.

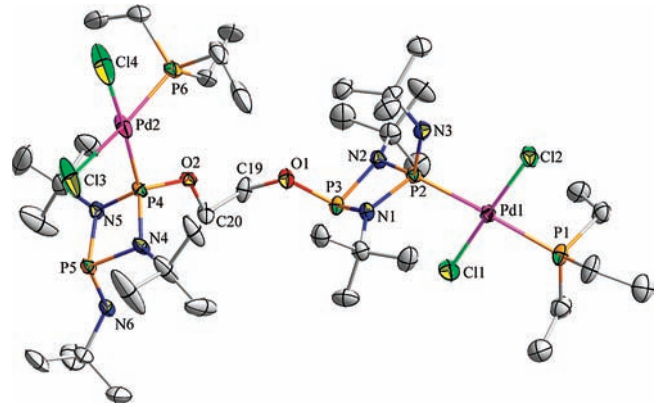

Figure 5. Molecular structure of complex [{Pd(PEt$_3$)Cl}$_2$-{^{t}BuHN(^{t}BuNP)$_2$OCH$_2$}$_2$] (**8**). Thermal ellipsoids are drawn at the 50% probability level. Hydrogen atoms have been omitted for clarity. Only one orientation of the disordered triethylphosphine ligand is shown.

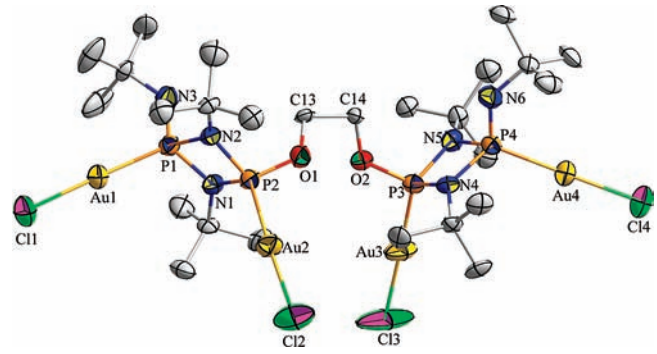

Figure 6. Molecular structure of complex [(AuCl)$_4${^{t}Bu-HN(^{t}BuNP)$_2$OCH$_2$}$_2$] (**9**). Thermal ellipsoids are drawn at the 50% probability level. Hydrogen atoms have been omitted for clarity. Only one orientation of the disordered *tert*-butyl groups is shown.

in both cyclic and acyclic diphosphazanes.[19] These trends are in good agreement with the structural data available for similar compounds such as Et$_2$C[CH$_2$OP(μ-N^{t}Bu)$_2$PNH^{t}Bu]$_2$, C[CH$_2$OP(μ-N^{t}Bu)$_2$PNH^{t}Bu]$_4$,[15] and O[CH$_2$OP(μ-N^{t}Bu)$_2$PNH^{t}Bu]$_2$.[16] The endocyclic P1−N1 and P1−N2 distances in **2** are 1.7317(16) and 1.7366(17) Å, respectively, while the corresponding P2−N1 (1.7012(17) Å) and P2−N2 (1.7132(16) Å) distances are slightly shorter but are still long compared to the exocyclic P1−N3 distance of 1.6637(18) Å. The average P−O bond distance (1.6383(14) Å) in **2** is

(19) Balakrishna, M. S.; Reddy, V. S.; Krishnamurthy, S. S.; Nixon, J. F.; Laurent, J. C. T. R. B. S. *Coord. Chem. Rev.* **1994**, *129*, 1–90.

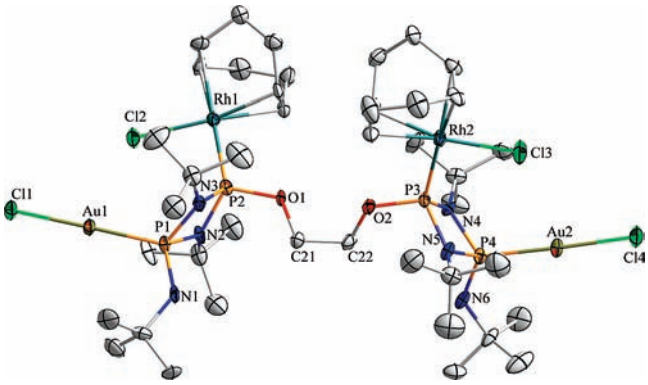

Figure 7. Molecular structure of complex [{Rh(COD)-Cl}$_2$(AuCl)$_2$\{^{t}BuHN(^{t}BuNP)$_2$O CH$_2$\}$_2$] (**10**). Thermal ellipsoids are drawn at the 50% probability level. Hydrogen atoms have been omitted for clarity. Only one orientation of the disordered *t*-butyl group is shown.

slightly longer than those in compounds **3** (1.5883(16)) and **4** (1.5868(17)) Å. The exocyclic P−N bonds shrinks further (av. 1.6249(17) Å) in the dichalcogenides, whereas the average endocyclic P−N bond distances in compounds **3** and **4** are 1.6808(17), 1.6782(17), and 1.6834(18) Å, respectively. The average P−S and P−Se distances are 1.9305(8) and 2.0542(5) Å, respectively. All of the P_2N_2 rings in **2**−**4** and in the remainder of the complexes discussed below are somewhat puckered with a folding along the N···N axis, as indicated by the dihedral angles between the corresponding NPN planes (Table 5). The torsion angle across the center linker of **2** (−O1−C13−C14−O2−) is 174.5(4)°, while in the noncentrosymmetric molecules of **3** and **4** (major conformer), it is 74.5(4)° and 82.6°, respectively. In **3** and **4**, the inner P═E (E = S, Se) vectors are approximately orthogonal, as indiated by the dihedral angles between the planes O1P2E2 and O2P3E3 of 83.3(3)° and 82.6(2)°, respectively. Additionally, weak C−H···O hydrogen bonds are seen in **2**, namely, C12−H12b···O1 (at 0.5 + *x*, −*y*, −0.5 + *z*; 2.51 Å, 155°) and C26−H26b···O2 (at −1 + *x*, *y*, *z*; 2.58 Å, 164°).

The structure of palladium complex **7** consists of four {PdCl(allyl)} moieties coordinated to the four phosphorus centers and adopts distorted square-planar geometries. The O−C−C−O dihedral angle is 177.6(5)° (anti conformation) with the P_2N_2 rings arranged in an antiparallel manner. The average Pd−P distance is 2.287(2) Å, and the exocyclic P−N bond distance is 1.654(6) Å, both of which do not deviate much from the free ligand values. In contrast, the endocyclic P−N bonds shrink considerably, with the inner phosphorus showing an average P−N bond distance of 1.679(6) Å, while for the outer phosphorus, it is 1.718(7) Å. In the molecular structure of **8**, only two alternate phosphorus atoms are coordinated to {$PdCl_2(PEt_3)$} moieties, and the palladium centers adopt typical square-planar geometries. Interestingly, the palladium(II) coordinated to the outer phosphorus adopts a trans geometry, but the palladium(II) bound to the inner phosphorus has a cis geometry. Although the {$PdCl_2(PEt_3)$} moiety is clearly too bulky for there to be one on each of the four phosphorus atoms of **2**, it is not obvious why the two present in **8** are coordinated to alternate phosphorus atoms. There should be no steric factors preventing both from coordinating to the outer phosphorus atoms, and were the ligand to adopt the anti conformation as seen in the centrosymmetric molecules of **3** and **4**, both should be able to coordinate to the inner phosphorus atoms. The observed regiochemistry as well as the different coordination geometries about palladium may reflect the mechanism of the formation of **8**. Thus, if the initial attack of **2** upon [PdCl(μ-Cl)PEt_3]$_2$ is by an outer phosphorus atom, which would be favored on steric grounds, followed by preferential cleavage of the Pd−Cl bond trans to the PEt_3 ligand, since the phosphine is above chloride in the trans-effect series, the palladium now coordinated to **2** will have a trans geometry, while the displaced (and presumably solvated) {$PdCl_2(PEt_3)$} fragment will have the chlorine ligands cis to one another. Since coordination of this fragment to the inner phosphorus of the same P_2N_2 ring is precluded on steric grounds, the closest available site would be the inner phosphorus on the other side of the molecule, and if this occurs more rapidly than isomerization, the cis geometry will be retained. The Pd2−P4 (2.2308(12) Å) and Pd2−P6 (2.280(2) Å) bond distances are ca. 0.1 and 0.03 Å shorter than Pd1−P2 (2.3307(15) Å) and Pd1−P1 (2.3133(16) Å), respectively, which may be due to the stronger π-acceptor nature of the cyclodiphosphazane ligand **2** as compared to PEt_3. The −O−C−C−O− torsion angle is only 65.6(5)° despite the fact that Pd2 and the lone pair on the other inner phosphorus are pointing in nearly opposite directions. In addition, there is a weak N−H···Cl hydrogen bond, namely, N6−H6n···Cl4 (at *x*, 1.5 − *y*, −0.5 + *z*; 2.74 Å, 163°).

The molecular structure of complex **9** reveals that all four phosphorus atoms are coordinated to {AuCl} units and are arranged in a cis fashion, as indicated by the 65.0(5)° torsion angle of the O−C−C−O linker and by the 63.1(3)° dihedral angle between the Au2P2O1 and Au3P3O2 planes. The average Au−P bond distance is 2.204(2) Å, with terminal Au−P bonds to the outer phosphorus atoms being slightly shorter than those to the inner phosphorus atoms. The Cl−Au−P (ca. 177.2 (1)°) bond angles are slightly less than that in [Ph_3PAuCl] (179.63°).[20] Although the gold atoms are arranged in a cis manner, there is no intramolecular aurophilic interaction, which is evident from the Au1···Au2 and Au3···Au4 distances of 5.243(1) and 5.226(1) Å, respectively. In addition, there are no intermolecular Au···Au interactions. The P−N and P−O bond distances in **9** are comparable to those in complexes **7** and **8**. Three of the four chlorine atoms participate in weak Cl···H−C hydrogen bonding, namely, Cl1···H14b−C14 (at 1 − *x*, 0.5 + *y*, 2 − *z*; 2.74 Å, 145°), Cl2···H20a−C20 (at *x*, *y*, 1 + *z*; 2.70 Å, 154°), and Cl4···H13b−C13 (at −*x*, −0.5 + *y*, 1 − *z*; 2.85 Å, 137°).

Crystals of **10** suitable for X-ray diffraction studies were obtained from a dichloromethane solution at room temperature. The core structure of **10** consists of {Rh(COD)Cl} moieties coordinated to the inner phosphorus atoms, with the outer phosphorus atoms coordinated to {AuCl} units. The gold centers have linear geometries, and the rhodium

(20) She, L.; Li, X.; Sun, H.; Ding, J.; Frey, M.; Klein, H.-F. *Organometallics* **2007**, *26*, 566–570.

Table 1. Crystallographic Information for **2**−**4** and **7**−**10**

	2	**3**	**4**	**7**	**8**	**9**	**10**
formula	$C_{26}H_{60}N_6O_2P_4$	$C_{26}H_{60}N_6O_2P_4S_4$	$C_{26}H_{60}N_6O_2P_4$ Se_4	$C_{40}H_{80}Cl_{10}N_6O_2P_4Pd_4$	$C_{38}H_{90}Cl_4N_6O_2P_6Pd_2$	$C_{26.5}H_{61}Au_4Cl_5N_6O_2P_4$	$C_{42}H_{84}Au_2Cl_4N_6O_2P_4Rh_2$
fw	612.68	740.96	928.52	1581.16	1203.62	1584.83	1570.59
cryst syst	monoclinic	triclinic	triclinic	triclinic	monoclinic	monoclinic	monoclinic
space group	*Pn*	$P\bar{1}$	$P\bar{1}$	$P\bar{1}$	$P2_1/c$	$P2_1$	$P2_1/n$
a, Å	9.760(1)	9.829(7)	9.830(1)	13.570(2)	18.354(1)	9.783(1)	14.156(2)
b, Å	11.932(1)	17.825(1)	17.953(2)	15.323(2)	18.173(1)	18.779(2)	19.090(3)
c, Å	15.511(2)	17.946(1)	18.240(2)	16.071(2)	19.685(1)	14.044(2)	21.947(3)
α, deg	90	106.334(1)	106.096(2)	75.354(2)	90	90	90
β, deg	94.896(2)	95.145(1)	95.848(2)	88.701(2)	117.370(1)	104.775(2)	107.241(1)
γ, deg	90	96.329(1)	95.696(2)	78.607(2)	90	90	90
V, Å^3	1799.8(3)	2974.8(3)	3049.2(6)	3168.1(7)	5830.9(5)	2494.8(5)	5664.4(14)
Z	2	3	3	2	4	2	4
ρ_{calc}, g cm^{-3}	1.131	1.241	1.517	1.658	1.371	2.110	1.842
μ(Mo Kα), mm^{-1}	0.240	0.432	3.798	1.676	0.999	12.150	6.076
F (000)	668	1194	1410	1584	2504	1478	3080
T (K)	100(2)	100(2)	100(2)	100(2)	100(2)	100(2)	110(2)
2*θ* range, deg	2.2−28.3	1.2−28.0	2.1−28.7	2.1−23.3	2.1−28.4	2.2−28.3	1.4−26.4
GOF (F^2)	1.03	1.04	1.04	1.02	1.08	1.02	1.04
R_1	0.0388	0.0418	0.0282	0.0557	0.0669	0.0430	0.0582
wR_2	0.0915	0.1084	0.0665	0.1608	0.1463	0.1094	0.1303

Table 2. Selected Bond Distances (Å) and Bond Angles (deg) for **2**−**4**

bond distances (Å)		bond angles (deg)	
	Compound **2**		
P1−N1	1.7317(16)	N1−P1−N2	79.77(8)
P1−N2	1.7366(17)	N1−P2−N2	81.29(8)
P1−N3	1.6637(18)	P1−N1−P2	98.57(9)
P2−N1	1.7012(17)	P1−N2−P2	97.92(9)
P2−N2	1.7132(16)	N1−P1−N3	105.70(8)
P2−O1	1.6383(14)	N4−P3−N5	81.23(8)
C13−O1	1.429(2)	N4−P4−N5	79.73(8)
C13−C14	1.497(3)		
	Compound **3**		
S1−P1	1.9405(8)	N2−P1−N3	82.86(8)
S2−P2	1.9293(7)	N2−P2−N3	84.52(8)
S5−P5	1.9453(8)	P1−N3−P2	95.06(8)
S6−P6	1.9195(7)	P1−N2−P2	94.88(8)
P1−N1	1.6241(16)	S1−P1−N1	108.40(7)
P1−N2	1.7030(16)	S2−P2−O1	113.08(6)
P2−N2	1.6759(17)	S4−P4−N4	114.85(7)
P2−O1	1.5862(16)	S3−P3−O2	112.18(6)
P5−N7	1.6266(16)	P5−N8−P6	95.89(8)
	Compound **4**		
Se1−P1	2.0741(6)	N1−P1−N2	82.72(8)
Se2−P2	2.0979(7)	N1−P2−N2	84.79(8)
Se3−P3	2.1115(7)	Se2−P2−O1	113.32(6)
Se5−P5	2.1016(6)	Se3−P3−O2	114.13(6)
Se6−P6	2.0735(6)	N4−P3−N5	84.40(8)
P1−N2	1.6941(17)	Se1−P1−N3	115.30(7)
P1−N3	1.6326(18)	Se6−P6−O3	112.18(6)
P1−N1	1.7068(18)	Se5−P5−N9	108.97(7)
P2−O1	1.5923(18)		

Table 3. Selected Bond Distances (Å) and Bond Angles (deg) for **7** and **8**

bond distances (Å)		bond angles (deg)	
	Compound **7**		
av. Pd−P	2.287(2)	Cl2−Pd1−P1	95.88(7)
av. Pd−Cl	2.378(2)	Cl1−Pd2−P2	100.56(7)
av. Pd−C	2.159(2)	Cl3−Pd3−P3	98.69(7)
P1−N1	1.725(7)	Cl4−Pd4−P4	96.96(7)
P1−N2	1.724(6)	N1−P1−N2	81.1(3)
P1−N3	1.654(6)	N1−P2−N2	83.8(3)
P2−N1	1.678(6)		
P2−N2	1.681(7)		
P2−O1	1.618(6)		
P3−O2	1.617(5)		
P3−N4	1.679(7)		
P3−N5	1.678(6)		
P4−N6	1.654(6)		
P4−N5	1.716(7)		
P4−N4	1.708(6)		
	Compound **8**		
Pd1−Cl1	2.3053(13)	Cl1−Pd1−Cl2	177.17(6)
Pd1−Cl2	2.3000(13)	Cl1−Pd1−P1	90.76(5)
Pd1−P1	2.3133(16)	Cl1−Pd1−P2	88.91(5)
Pd1−P2	2.3307(15)	Cl2−Pd1−P1	87.49(5)
Pd2−Cl3	2.327(2)	P1−Pd1−P2	177.13(5)
Pd2−Cl4	2.3599(17)	Cl3−Pd2−Cl4	89.36(8)
Pd2−P4	2.2308(12)	Cl3−Pd2−P4	85.32(6)
Pd2−P6	2.280(2)	Cl3−Pd2−P6	173.93(6)
P2−N1	1.691(4)	P4−Pd2−P6	100.75(6)
P2−N2	1.690(4)		
P2−N3	1.635(4)		
P3−O1	1.651(4)		
P3−N1	1.706(4)		
P3−N2	1.720(4)		
P4−O2	1.598(4)		
P4−N4	1.652(4)		
P4−N5	1.659(4)		
P5−N4	1.754(4)		
P5−N5	1.758(4)		
P5−N6	1.647(4)		

centers are in distorted square-planar environments. The P1−Au−Cl1 (175.2(1)°) and P4−Au−Cl4 (175.7(1)°) bond angles are ca. 4σ less than that in [Ph_3PAuCl] (179.63°).[20] The Rh−C bond distances are in the range of 2.12(1)−2.26(1) Å. The Au−P and Au−Cl bond distances are similar to those in complex **6**. The Rh1−P2 (2.239(3) Å) and Rh2−P3 (2.246(3) Å) bond distances are comparable to those in [RhCl(COD){^{t}BuNP(OC$_6$H$_4$OMe-*o*)}$_2$] (2.244(7) Å).[21] In **10**, the −O−C−C−O− torsion angle is 92.7(5)°, while the dihedral angle between the Rh1P2O1 and Rh2P3O2 planes is 60.8(3)°. As in **8**, weak N−H···Cl hydrogen bonds are present in the crystal, namely, N1−H1n···Cl4 (at 1.5 − *x*, 0.5 + *y*, 0.5 − *z*; 2.74 Å, 161°) and N6−H6n···Cl1 (at 0.5 − *x*, −0.5 + *y*, 0.5 − *z*; 2.86 Å, 169°).

Conclusions

The reaction of *cis*-{Bu^{t}NH(^{t}BuNP)$_2$Cl} with ethylene glycol affords a bis(cyclodiphosphazane) containing four

(21) Chandrasekaran, P.; Mague, J. T.; Balakrishna, M. S. *Inorg. Chem.* **2005**, *44*, 7925–7932.

Table 4. Selected Bond Distances (Å) and Bond Angles (deg) for **9** and **10**

bond distances (Å)		bond angles (deg)	
	Compound **9**		
av. Au−P	2.204(2)	Cl1−Au1−P1	178.20(11)
av. Au−Cl	2.266(4)	Cl2−Au2−P2	172.73(12)
P1−N3	1.601(9)	Cl3−Au3−P3	178.33(17)
P1−N2	1.698(8)	Cl4−Au4−P4	179.65(11)
P1−N1	1.703(8)	Au2−P2−O1	104.7(3)
P2−O1	1.579(6)	Au3−P3−O2	106.8(2)
P2−N1	1.676(8)	Au1−P1−N3	114.8(3)
P2−N2	1.670(8)	Au4−P4−N6	114.4(3)
P3−O2	1.584(6)		
P3−N5	1.675(7)		
P3−N4	1.688(8)		
P4−N4	1.711(7)		
P4−N5	1.704(8)		
P4−N6	1.608(9)		
	Compound **10**		
Au1−Cl1	2.301(3)	Cl1−Au1−P1	175.18(10)
Au1−P1	2.217(3)	Cl4−Au2−P4	175.70(10)
Au2−Cl4	2.293(3)	Cl2−Rh1−P2	88.35(10)
Au2−P4	2.218(3)	Cl3−Rh2−P3	89.21(10)
Rh1−Cl2	2.354(3)	Cl2−Rh1−C13	161.7(3)
Rh1−P2	2.239(3)	Cl2−Rh1−C14	159.1(3)
Rh2−P3	2.245(3)	P2−Rh1−C13	93.4(3)
Rh2−Cl3	2.347(3)		
P1−N1	1.627(9)		
P1−N2	1.696(8)		
P1−N3	1.698(8)		
P2−O1	1.604(6)		
P2−N2	1.690(9)		
P2−N3	1.711(8)		
P3−O2	1.610(7)		
P3−N4	1.688(8)		
P3−N5	1.672(9)		
P4−N4	1.697(8)		
P4−N5	1.704(8)		
P4−N6	1.622(9)		

Table 5. Puckering of the Cyclodiphosphazane P_2N_2 Rings

compound	plane 1	plane 2	dihedral angle (deg)
2	P1N1N2	P2N1N2	15.5(2)
	P3N4N5	P4N4N5	21.3(2)
3	P1N2N3	P2N2N3	16.6(1)
	P3N5N6	P4N5N6	7.4(1)
	P5N8N9	P6N8N9	8.4(1)
4	P1N1N2	P2N1N2	6.2(1)
	P3N4N5	P4N4N5	16.6(1)
	P5N7N8	P6N7N8	7.9(1)
7	P1N1N2	P2N1N2	5.8(1)
	P3N4N5	P4N4N5	5.5(1)
8	P2N1N2	P3N1N2	15.5(2)
	P4N4N5	P5N4N5	14.2(1)
	P1N1N2	P2N1N2	8.9(2)
	P3N4N5	P4N4N5	7.9(2)
10	P1N2N3	P2N2N3	14.6(4)
	P3N4N5	P4N4N5	11.8(4)

phosphorus(III) atoms in quantitative yield. The bis(cyclodiphosphazane) reacts with elemental sulfur and selenium to give tetrakis(chalcogenide) derivatives and with $[Rh(COD)Cl]_2$ to form a dimetallic complex involving the coordination of {RhCl(COD)} moieties to only the inner phosphorus centers. A similar reaction with $[PdCl_2(PEt_3)]_2$ also produces a dimetallic complex but involving alternating phosphorus centers with the resulting regiochemistry possibly due to a combination of the steric bulk of the PEt_3 ligand and the course of the substitution process at palladium. However, similar reactions of the bis(cyclodiphosphazane) with $AuCl(SMe_2)$ and $[Pd(\eta^3\text{-}C_3H_5)Cl]_2$ led to the isolation of tetrametallic complexes. The tetrametallic palladium(II) complex, $[\{Pd(\eta^3\text{-}C_3H_5)Cl\}_4\{^tBuHN(^tBuNP)_2OCH_2\}_2]$, is a rare example of a species having four allyl-palladium moieties without palladium−palladium interactions. Presently, we are examining the coordinating ability of **2** both as an anionic and neutral ligand to make binuclear complexes with disparate metals and also the catalytic activity of platinum metal complexes in organic synthesis.

Experimental Section

General Procedures. All manipulations were performed under rigorously anaerobic conditions using Schlenk techniques. All of the solvents were purified by conventional procedures and distilled prior to use.[22] The compounds *cis*-$\{^tBuHN(^tBuNP)_2Cl\}$ (**1**),[13] $[Rh(COD)Cl]_2$,[23] $[PdCl_2(PEt_3)]_2$,[24] $[Pd(\eta^3\text{-}C_3H_5)Cl]_2$,[25] and $AuCl(SMe_2)$[26] were prepared according to the published procedures. Other chemicals were obtained from commercial sources and purified prior to use.

Instrumentation. The ^1H and $^{31}P\{^1H\}$ NMR (δ in parts per million) spectra were recorded using a Varian VXR 300 or VXR 400 spectrometer operating at the appropriate frequencies using TMS and 85% H_3PO_4 as internal and external references, respectively. The microanalyses were performed using a Carlo Erba Model 1112 elemental analyzer. The melting points were observed in capillary tubes and are uncorrected.

Synthesis of $\{^tBuHN(^tBuNP)_2OCH_2\}_2$ (2). A mixture of ethylene glycol (0.65 g, 10.4 mmol) and triethylamine (2.3 g, 24 mmol) in diethyl ether (20 mL) was added dropwise to an ice-cold solution of *cis*-$\{^tBuHN(^tBuNP)_2Cl\}$ (6.49 g, 21 mmol) also in diethyl ether (80 mL). After the completion of the addition, a catalytic amount (10 mg) of 4-N,N′-dimethylaminopyridine in 5 mL of THF was added, and the reaction mixture was stirred for 12 h at room temperature and then filtered through celite. All the solvents were removed under a vacuum to obtain a white solid, which was crystallized from a dichloromethane and acetonitrile (1:2) mixture. Yield: 93% (5.93 g, 9.67 mmol). Mp: 144−146 °C. Anal. calcd for $C_{26}H_{60}P_4O_2N_6$: C, 50.97; H, 9.87; N, 13.72. Found: C, 50.99; H, 9.72; N, 13.91. ^1H NMR (400 MHz, $CDCl_3$): δ 1.27 (d, ^tBu, $^3J_{PH} = 1.6$, 18H), 1.30 (s, ^tBu, 36H), 2.93 (d, *NH*, $^2J_{PH} = 8.8$, 2H), 3.84 (m, CH_2, 4H). $^{31}P\{^1H\}$ NMR (162 MHz, $CDCl_3$): δ 112.7 (s), 92.4 (s). MS (EI): m/z 613.69 $[M + 1]^+$.

Synthesis of $\{^tBuHN(^tBuNP(S))_2OCH_2\}_2$ (3). A mixture of sulfur (0.021 g, 0.65 mmol) and **2** (0.1 g, 0.16 mmol) in 15 mL of toluene was refluxed for 24 h. The reaction mixture was cooled to room temperature, filtered through celite, and concentrated to 5 mL under a vacuum. The solution was diluted with 5 mL of acetonitrile and stored at room temperature for 24 h to give analytically pure colorless crystals of **3**. Yield: 84% (0.1 g, 0.13 mmol). Mp: 214−216 °C. Anal. calcd for $C_{26}H_{60}O_2P_4N_6S_4$: C, 42.14; H, 8.16; N, 11.34; S, 17.31. Found: C, 42.24; H, 8.20; N, 11.36; S, 17.28. ^1H NMR (400 MHz, $CDCl_3$): δ 1.43 (d, ^tBu, $^3J_{PH} = 0.8$, 18H), 1.59 (s, ^tBu, 36H), 3.12 (d, *NH*, $^2J_{PH} = 8.8$, 2H), 4.30 (m, CH_2,

(22) Armarego, W. L. F.; Perrin, D. D. *Purification of Laboratory Chemicals*, 4th ed.; Butterworth-Heinemann: Jordan Hill, Oxford, UK, 1996.
(23) Giodrano, G.; Carbtree, R. H. *Inorg. Synth.* **1990**, *28*, 88–89.
(24) Baratta, W.; Pregosin, P. S. *Inorg. Chim. Acta* **1993**, *209*, 85–87.
(25) Tatsuno, Y.; Yoshida, T.; Otsuka, S. *Inorg. Synth.* **1990**, *28*, 342–343.
(26) Brandys, M.; Jennings, M. C.; Puddephatt, R. J. *J. Chem. Soc., Dalton Trans.* **2000**, 4601–4606.

4H). ^{31}P{^{1}H} NMR ($CDCl_3$, 162 MHz): δ 37.5 (d, $^2J_{PP}$ = 16.2), 51.4 (d, $^2J_{PP}$ = 16.2). MS (EI): *m/z* 741.58 $[M + 1]^+$.

Synthesis of {^{t}BuHN(^{t}BuNP(Se))$_2$OCH$_2$}$_2$ (4). This procedure is similar to that of **3** using selenium (0.052 g, 0.65 mmol). Yield: 91% (73.4 mg, 0.08 mmol). Mp: 208 °C (dec). Anal. calcd for $C_{26}H_{60}O_2P_4N_6Se_4$: C, 33.63; H, 6.51; N, 9.05. Found: C, 33.58; H, 6.57; N, 9.34. ^{1}H NMR (400 MHz, $CDCl_3$): δ 1.45 (s, ^{t}*Bu*, 18H), 1.65 (s, ^{t}*Bu*, 36H), 3.47 (d, *NH*, $^2J_{PH}$ = 11.6, 2H), 4.32 (m, *CH*$_2$, 4H). ^{31}P{^{1}H} NMR ($CDCl_3$, 162 MHz): δ 24.4 (d, $^1J_{SeP}$ = 895.5, $^2J_{PP}$ = 18.0), 45.8 (d, $^1J_{SeP}$ = 936.6, $^2J_{PP}$ = 18.0). MS (EI): *m/z* 930.69 $[M]^+$.

Synthesis of {^{t}BuHNP(μ-^{t}BuN)$_2$P(Se)OCH$_2$}$_2$ (5). A mixture of selenium (0.019 g, 0.24 mmol) and **2** (0.075 g, 0.12 mmol) in 10 mL of toluene was stirred at room temperature for 8 h. The reaction mixture was filtered and concentrated to 2 mL diluted with 5 mL of petroleum ether and stored at −30 °C for a day to afford an analytically pure colorless crystalline product. Yield: 92% (0.086 g, 0.11 mmol). Mp: 120−122 °C. Anal. calcd for $C_{26}H_{60}O_2P_4N_6Se_2$: C, 40.52; H, 7.85; N, 10.91. Found: C, 40.71; H, 7.76; N, 11.10. ^{1}H NMR (400 MHz, $CDCl_3$): δ 1.30 (d, ^{t}*Bu*, $^3J_{PH}$ = 1.2, 18H), 1.44 (s, ^{t}*Bu*, 36H), 3.02 (d, *NH*, $^2J_{PH}$ = 7.6, 2H), 4.27 (m, *CH*$_2$, 4H). ^{31}P{^{1}H} NMR ($CDCl_3$, 162 MHz): δ 46.0 (d, $^1J_{SeP}$ = 874.3, $^2J_{PP}$ = 12.3), 78.6 (d, $^2J_{PP}$ = 12.3). MS (EI): *m/z* 772.78 $[M]^+$.

Synthesis of [{^{t}BuHNP(μ-^{t}BuN)$_2$P(Rh(COD)Cl)OCH$_2$}$_2$] (6). A solution of $[Rh(COD)Cl]_2$ (0.032 g, 0.065 mmol) in 10 mL of dichloromethane was added dropwise to a dichloromethane (10 mL) solution of **2** (0.04 g, 0.065 mmol) at room temperature. The reaction mixture was stirred for 4 h, concentrated to 5 mL, diluted with 5 mL of diethyl ether, and kept at −30 °C for a day to give a pure pale yellow crystalline product. Yield: 82% (0.06 mg, 0.05 mmol). Mp: 172−174 °C. Anal. calcd for $C_{42}H_{84}P_4N_6O_2Rh_2Cl_2$: C, 45.62; H, 7.66; N, 7.60. Found: C, 45.36; H, 7.40; N, 7.72. ^{1}H NMR (400 MHz, $CDCl_3$): δ 1.34 (d, ^{t}*Bu*, $^3J_{PH}$ = 1.2, 18H), 1.55 (s, ^{t}*Bu*, 36H), 3.02 (d, *NH*, $^2J_{PH}$ = 6.4, 2H), 3.79 (m, *CH*$_2$, 4H), 2.09 (m, *CH*$_2$, COD, 4H), 2.34 (m, *CH*$_2$, COD, 4H), 3.81(br s, *CH*, COD, 2H), 5.51(br s, *CH*, COD, 2H). ^{31}P{^{1}H} NMR ($CDCl_3$, 162 MHz): δ 90.8 (s), 91.9 (d, $^1J_{RhP}$ = 219.3). MS (EI): *m/z* 1105.30 $[M + 1]^+$.

Synthesis of [{Pd(η^3-C$_3$H$_5$)Cl}$_4${^{t}BuHN(^{t}BuNP)$_2$OCH$_2$}$_2$] (7). A solution of $[Pd(\eta^3\text{-}C_3H_5)Cl]_2$ (0.05 g, 0.14 mmol) in 10 mL of dichloromethane was added dropwise to a well-stirred dichloromethane (10 mL) solution of **2** (0.042 g, 0.068 mmol) at room temperature. The reaction mixture was stirred for 4 h, concentrated to 5 mL, diluted with 5 mL of diethyl ether, and stored at −30 °C for a day to afford a pure pale yellow crystalline product of **7**. Yield: 81% (0.07 g, 0.05 mmol). Mp: 168 °C (dec). Anal. calcd for $C_{38}H_{80}O_2P_4N_6Pd_4Cl_4$: C, 33.95; H, 6.00; N, 6.25. Found: C, 34.04; H, 5.82; N, 6.13. ^{1}H NMR (400 MHz, $CDCl_3$): δ 1.45 (s, ^{t}*Bu*, 18H), 1.58 (s, ^{t}*Bu*, 18H), 1.62 (s, ^{t}*Bu*, 18H), 2.90 (br d), 4.0 (br m), 3.57−5.64 (br m, allyl). ^{31}P{^{1}H} NMR ($CDCl_3$, 162 MHz): δ 76.4 (s), 77.6 (s), 118.4 (s), 118.6 (s). MS (EI): *m/z* 1309.28 $[M - Cl]^+$.

Synthesis of [{PdCl$_2$(PEt$_3$)}$_2${^{t}BuHN(^{t}BuNP)$_2$OCH$_2$}$_2$] (8). A solution of $[PdCl_2(PEt_3)]_2$ (0.04 g, 0.04 mmol) in 10 mL of dichloromethane was added dropwise to a dichloromethane (10 mL) solution of **2** (0.025 g, 0.04 mmol) at room temperature. The reaction mixture was stirred for 4 h, concentrated to 5 mL, diluted with 5 mL of diethyl ether, and stored at room temperature for three days to form a pale yellow crystalline product. Yield: 95% (0.047 g, 0.04 mmol). Mp: 190 °C (dec). Anal. calcd for $C_{38}H_{90}P_6N_6O_2Pd_2Cl_4$: C, 37.92; H, 7.54; N, 6.98. Found: C, 37.99; H, 7.52; N, 7.02. ^{1}H NMR (400 MHz, $CDCl_3$): δ 1.34 (s, ^{t}*Bu*, 9H), 1.40 (s, ^{t}*Bu*, 9H), 1.53 (s, ^{t}*Bu*, 18H), 1.56 (s, ^{t}*Bu*, 18H), 2.80 (d, *NH*, $^2J_{PH}$ = 4.8, 2H), 4.04 (m, *CH*$_2$, 4H), 1.16 (t, *Et*, 9H), 1.20 (t, *Et*, 9H), 1.86 (m, *Et*, 6H), 2.07 (m, *Et*, 6H). ^{31}P{^{1}H} NMR ($CDCl_3$, 162 MHz): δ 20.2 (dd, $^2J_{PP}$ = 711, $^5J_{PP}$ = 8.9), 29.3 (d, $^2J_{PP}$ = 14.6), 59.2 (dd,$^2J_{PP}$ = 711, $^2J_{PP}$ = 6.6), 72.8 (dd, $^2J_{PP}$ = 14.4, $^2J_{PP}$ = 8.3), 92.0 (d, $^2J_{PP}$ = 7.8), 126.9 (dd, $^2J_{PP}$ = 6.8, $^5J_{PP}$ = 8.9).

Synthesis of [Au$_4$Cl$_4${^{t}BuHN(^{t}BuNP)$_2$OCH$_2$}$_2$] (9). A dichloromethane (8 mL) solution of $[AuCl(SMe_2)]$ (0.05 g, 0.17 mmol) was added slowly to a solution of **2** (0.026 g, 0.04 mmol) in dichloromethane (10 mL) at room temperature. The mixture was kept undisturbed for 2 days to give analytically pure crystals of **9**. Yield: 96% (0.063 g, 0.04 mmol). Mp: >250 °C. Anal. calcd for $C_{26}H_{60}O_2P_4N_6Au_4Cl_4$: C, 20.25; H, 3.92; N, 5.49. Found: C, 20.36; H, 3.82; N, 5.57.

Synthesis of [{RhCl(COD)}$_2$Au$_2$Cl$_2${^{t}BuHN(^{t}BuNP)$_2$OCH$_2$}$_2$] (10). A solution of $[AuCl(SMe_2)]$ (0.011 g, 0.04 mmol) in 3 mL of dichloromethane was added slowly to a dichloromethane (10 mL) solution of **6** (0.02 g, 0.018 mmol) at room temperature. The reaction mixture was kept undisturbed for 24 h to give a yellow crystalline product of **10**. Yield: 90% (0.025 g, 0.016 mmol). Mp: 228 °C (dec). Anal. calcd for $C_{42}H_{84}P_4N_6O_2Rh_2Au_2Cl_4$: C, 32.12; H, 5.39; N, 5.35. Found: C, 31.92; H, 5.32; N, 5.41. MS (EI): *m/z* 930.69 $[M]^+$.

X-Ray Crystallography. A crystal of each of the compounds **2**−**4** and **7**−**10** suitable for X-ray crystal analysis was mounted in a Cryoloop with a drop of Paratone oil and placed in the cold nitrogen stream of the Kryoflex attachment of the Bruker APEX CCD diffractometer. Full spheres of data were collected using 606 scans in ω (0.3° per scan) at ϕ = 0, 120, and 240° or a combination of three sets of 400 scans in ω (0.5° per scan) at φ = 0, 90, and 180° plus two sets of 800 scans in φ (0.45° per scan) at ω = −30 and 210° under the control of the SMART software package[27a] or the APEX2 program suite.[27b] The raw data were reduced to F^2 values using the SAINT+ software,[28] and global refinements of unit cell parameters using 6680−9939 reflections chosen from the full data sets were performed. Multiple measurements of equivalent reflections provided the basis for empirical absorption corrections as well as corrections for any crystal deterioration during the data collection (SADABS[29]). The structures were solved by direct methods, or the positions of the heavy atoms were obtained from a sharpened Patterson function. All structures were refined by full-matrix least-squares procedures using the SHELX-TL program package.[30] Hydrogen atoms attached to carbon were placed in calculated positions and included as riding contributions with isotropic displacement parameters tied to those of the attached non-hydrogen atoms. Those attached to nitrogen were placed in locations derived from a difference map and also included as riding contributions as for the others. Initial attempts to obtain a unit cell for **10** were unsuccessful, so a set of 1448 reflections having $I/\sigma(I) > 10$ chosen from the full data were processed with CELL_NOW,[31] which showed that the crystal was twinned by a 180° rotation about *c**. Integration of the twinned data set was accomplished with the two-component version of SAINT+, as controlled by the two-component orientation file generated by CELL_NOW. Multiple measurements of equivalent reflections provided the basis for an empirical absorption correction as well as correction for any crystal deterioration during the data

(27) (a) *SMART*, version 5.625; Bruker-AXS: Madison, WI, 2000. (b) *APEX2*, version 2.1-0; Bruker-AXS: Madison, WI, 2006.
(28) *SAINT+*, versions 6.35A and 7.34A; Bruker-AXS: Madison, WI, 2002 and 2006.
(29) Sheldrick, G. M. *SADABS*, version 2.05 and 2007/2; University of Göttingen: Göttingen, Germany, 2002 and 2007.
(30) (a) *SHELXTL*, version 6.10; Bruker-AXS: Madison, WI, 2000 . (b) Sheldrick, G. M. *SHELXS97*; *SHELXL97*; University of Göttingen: Göttingen, Germany, 1997 .
(31) Sheldrick, G. M. *CELL_NOW*; University of Göttingen: Göttingen, Germany, 2005.

collection, which was applied with TWINABS[32] and which also extracted a set of F^2 values for the primary component of the twin. This was used for structure solution and preliminary refinement, while final refinement was accomplished using the full two-component data set. Also in the latter stages of refinement, it became evident that the *tert*-butyl group built on C35 is rotationally disordered, apparently over several sites. A reasonable model proved to be one involving two sites with the geometries restrained to be ideal. For **2**, the *tert*-butyl group attached to N1 is rotationally disordered over two well-resolved sites in the ratio 72:28. The two orientations were refined subject to restraints that their geometries be the same. In **4**, the two-carbon link (C13 and C14) between O1 and O2 in the molecule located in the general position is disordered over two well-resolved sites, as are Se1 and Se2. Refinement of the separate sites subject to the constraint that their occupancies sum to 1.0 and restraints of comparable geometry for the two orientations converged at a site occupancy ratio of 86:14. In **7**, the η^3-allyl groups attached to Pd2 and Pd4 are rotationally disordered over two alternate sites each. On Pd2, the occupancy ratio of the two sites is 54/46, while on Pd4 it is 70/30 following a refinement strategy analogous to that used for **4**. For one of the triethylphosphine ligands in **8**, the ethyl substituents were disordered over two approximately equally populated sites. These were refined with restraints comparable to those used for **4** and **7**. There appears to be a degree of disorder at the opposite end of the molecule, as indicated by the elongated displacement ellipsoids for many of its atoms, but it was not considered feasible to model this in more detail. Two of the *tert*-butyl groups in **9** (built on C5 and C19) are rotationally disordered with each showing a 3:2 occupancy ratio for the two sites. These were refined with restraints to approximate idealized geometry.

(32) Sheldrick, G. M. *TWINABS*, version 2007/2; University of Göttingen: Göttingen, Germany, 2007.

Acknowledgment. We are grateful to the Department of Science and Technology (DST), New Delhi, for financial support of this work through Grant SR/S1/IC-02/007. We also thank the Department of Chemistry Instrumentation Facilities, Bombay, for spectral and analytical data and J.T.M. thanks the Louisiana Board of Regents for purchase of the CCD diffractometer and the Chemistry Department of Tulane University for support of the X-ray laboratory.

Supporting Information Available: X-ray crystallographic files in CIF format for the structure determinations of **2**−**4** and **7**−**10**. This material is available free of charge via the Internet at http://pubs.acs.org.

IC801256H